

# Systematics of the low-energy electric dipole strength in the Sn isotopic chain

M. Markova<sup>a</sup>, P. von Neumann-Cosel<sup>b</sup>, E. Litvinova<sup>c,d,e</sup>

<sup>a</sup>Department of Physics, University of Oslo, N-0316 Oslo, Norway

<sup>b</sup>Institut fuer Kernphysik, Technische Universitaet Darmstadt, D-64289 Darmstadt, Germany

<sup>c</sup>Department of Physics, Western Michigan University, Kalamazoo, Michigan 49008, USA

<sup>d</sup>National Superconducting Cyclotron Laboratory, Michigan State University, East Lansing, Michigan 48824, USA

<sup>e</sup>GANIL, CEA/DRF-CNRS/IN2P3, F-14076 Caen, France

## Abstract

We present a systematic study of the mass dependence of the low-energy electric dipole strength (LEDS) in Sn isotopes in the range  $A = 111 - 124$  based on data obtained with the Oslo method and with relativistic Coulomb excitation in forward-angle ( $p, p'$ ) scattering. The combined data cover an energy range of 2 – 20 MeV which permits, with minimal assumptions, a decomposition of the total strength into the contribution from the low-energy tail of the isovector giant dipole resonance (IVGDR) and possible resonance-like structures on top of it. In all cases, a resonance peaked at about 8.3 MeV is observed, exhausting an approximately constant fraction of the Thomas-Reiche-Kuhn (TRK) sum rule with a local maximum at  $^{120}\text{Sn}$  which might be related to shell structure effects. For heavier isotopes ( $A \geq 118$ ) a consistent description of the data requires the inclusion of a second resonance centered at 6.5 MeV, representing the isovector response of the pygmy dipole resonance (PDR). Its strength corresponds to a small fraction of the total LEDS only and shows an approximately linear dependence on mass number. The experimental results are also compared to ab initio-based microscopic calculations to investigate the importance of an inclusion of quasiparticle vibration coupling (qPVC) for a realistic description of the LEDS.

**Keywords:**  $^{111-124}\text{Sn}$ , Oslo method, ( $p, p'$ ) scattering, Low-energy electric dipole strength

## 1. Introduction

The observation of a resonance-like structure in the electric dipole response of heavy nuclei at energies around or below the neutron threshold, commonly termed pygmy dipole resonance (PDR), has been a topic leading to considerable experimental and theoretical activities in recent years [1, 2, 3, 4]. The interest has been triggered by attempts to interpret the underlying structure and also investigate its impact on the cross sections of ( $n, \gamma$ ) reactions relevant to a deeper understanding of the nucleosynthesis of heavy elements [5]. Qualitatively, all mean-field-based models predict the appearance of such a mode, however, with a broad range of strengths and energy centroids depending on a chosen interaction, a model space, and possible extensions beyond the random phase approximation (RPA) level.

Many theoretical studies interpret the PDR to arise from neutron skin oscillations, which implies a dependence of the PDR strength on neutron excess [6, 7, 8, 9, 10, 11, 12]. Accordingly, some models predict a correlation of the PDR strength with neutron skin thickness, which in turn suggests that information on the symmetry energy parameters of neutron-rich matter can be derived (see e.g. [7, 9]). These claims, however, have been questioned [13, 14, 15, 16, 17]. The neutron skin oscillation interpretation has been mainly based on a specific form of

transition densities in the energy region of the PDR with an approximately isoscalar (IS) radial dependence in the interior and a peak of the neutron density at the surface. The dominance of the neutron character of the  $E1$  transitions forming the PDR is experimentally confirmed by studies of the IS response with ( $\alpha, \alpha'\gamma$ ) [18, 19] and ( $^{17}\text{O}, ^{17}\text{O}'\gamma$ ) [20, 21] reactions. However, Ref. [22] points out that all experimental signatures of the PDR, viz., large ground-state branching ratios, large isovector (IV) strengths (with respect to average  $B(E1)$  transition strengths at low excitation energies), significant IS strengths, as well as the characteristic form of the transition density in heavy nuclei, are consistent with an interpretation as a low-energy IS toroidal mode. The recent first experimental demonstration [23] of the toroidal nature of low-energy  $E1$  transitions with all the experimental signatures quoted above, albeit in a  $N \approx Z$  nucleus, and successful description of these data by models predicting a dominantly toroidal nature of the PDR further challenge the neutron skin oscillation picture.

The best suited case for a systematic investigation of a dependence of PDR properties on neutron excess is the Sn isotope chain between  $A = 100$  and 132. Despite covering a variation from neutron shell closure to mid-shell, the proton shell closure stabilizes the g.s. features leading to similar low-energy structure along the chain. Thus, theoretical work has been focused on the Sn chain, attempting to predict the evolution of the PDR photoabsorption cross sections with neutron excess in order to test a possible relation to the neutron skin thickness [6, 7, 8, 9, 10, 11, 12, 13, 17]. However, many of these studies

Email addresses: maria.markova@fys.uio.no (M. Markova),  
vnc@ikp.tu-darmstadt.de (P. von Neumann-Cosel),  
elena.litvinova@wmich.edu (E. Litvinova)

use a summed strength below some cutoff energy to represent the PDR photoabsorption cross sections, despite this approach not being supported by the data. Experimental studies of the IS component of the PDR have demonstrated an isospin splitting (for  $^{124}\text{Sn}$  see [19, 21, 24]), where good correspondence between transitions excited in the IS and IV response is observed in a confined energy region at lower excitation energies, while at higher excitation energies the IV response dominates.

Furthermore, a comparison of photoabsorption cross sections in  $^{112,116,120,124}\text{Sn}$  [25, 26] deduced from Coulomb excitation in forward-angle ( $p, p'$ ) scattering [27] and from the ( $\gamma, \gamma'$ ) reaction [28, 29] shows good agreement in the energy region where the IS strength was also found, but large differences at higher excitation energies. The strengths deduced from the ( $\gamma, \gamma'$ ) experiments depend on the g.s. branching ratio [30]. The dramatic reduction compared to the ( $p, p'$ ) results points to a complex structure of the excited states with small g.s. branching ratios, suggesting that they rather belong to the low-energy tail of the IVGDR. Thus, a significant part of the low-energy photoabsorption strength is *not* related to the PDR. This interpretation has recently been confirmed by a new  $^{120}\text{Sn}(\gamma, \gamma')$  experiment [31], where the contributions from the statistical decay were additionally extracted.

Here we present a systematic study of the LEDS in Sn isotopes with mass numbers from 111 to 124. It is based on a new set of Gamma Strength Functions (GSFs) from  $\gamma$  decay after light-ion-induced compound reactions (the so-called Oslo method) [32, 33, 34] combined with a recent study of stable even-mass isotopes with relativistic Coulomb excitation in the ( $p, p'$ ) reaction [25, 35]. The GSFs are directly related to the photoabsorption cross sections, provided the Brink-Axel hypothesis [36, 37] also holds for the LEDS. This seems to be the case for Sn isotopes [32, 33, 34]. The combined data sets allow a decomposition of the LEDS with minimal assumptions, providing information on the evolution of the PDR strength and other components with neutron excess. The extraction of the GSFs from the Oslo data and a critical investigation of the assumptions underlying the decomposition and possible variants thereof are discussed in detail in Ref. [38]. The experimental GSFs are also compared to ab initio-based microscopic calculations to investigate the importance of an inclusion of quasiparticle vibration coupling (qPVC) for a description of the LEDS.

## 2. Experimental data

GSFs extracted with the Oslo method are available for  $^{111-113,116-122,124}\text{Sn}$ . They typically cover a  $\gamma$  energy range from about 2 MeV to 1–2 MeV below the respective neutron thresholds ( $S_n$ ). The results for  $^{111-113}\text{Sn}$ ,  $^{116}\text{Sn}$ , and  $^{118}\text{Sn}$  were obtained with a custom-designed Si telescope ring (SiRi) [39] combined with the CACTUS  $\gamma$  ball [40] made of 28  $5'' \times 5''$  NaI detectors. New experiments were performed for  $^{117,119,120,124}\text{Sn}$  using the OSCAR detector system [41, 42], consisting of 30 large-volume LaBr  $\gamma$  detectors providing superior efficiency, timing, and energy resolution compared to the previous experimental setup. Therefore, the new data for  $^{117,119}\text{Sn}$  supersede

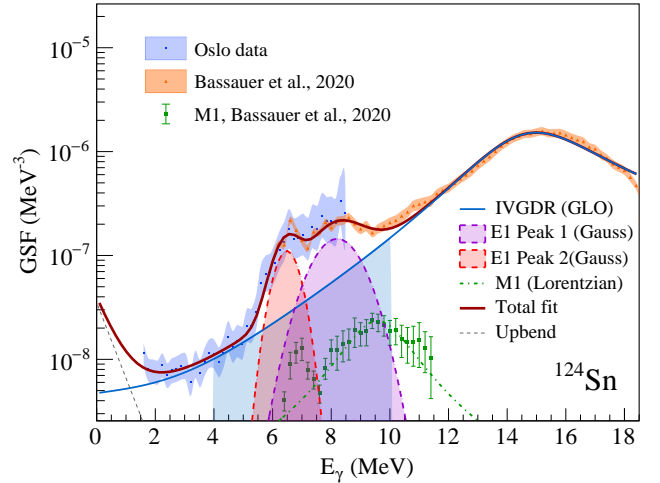


Figure 1: Decomposition of the experimental GSF of  $^{124}\text{Sn}$ . The Oslo data (blue data points and error) are shown together with the ( $p, p'$ ) results (orange data points and error band)[25]. The fit of the IVGDR with the GLO model, Eq. (1), is presented as solid blue line. The low-lying  $E1$  components are shown as shaded red and violet areas. The  $M1$  data from the ( $p, p'$ ) experiment [25] and the corresponding Lorentzian fit are given by the green data points and the dashed line, respectively. The upbend at low  $\gamma$  energies is described by the grey dashed line. The total fit is shown as solid magenta line.

previous results. Details of the consistent extraction of nuclear level densities and GSFs are described in Ref. [38].

An independent set of GSFs for the even-mass isotopes  $^{112-120,124}\text{Sn}$  is available from relativistic Coulomb excitation in the ( $p, p'$ ) reaction at extreme forward angles [25]. They agree in all cases with the Oslo method results within the respective error bars. This implies that the Brink-Axel hypothesis underlying the Oslo method and controversially discussed for the LEDS (see e.g. Refs. [43, 44, 45, 46]) holds in case of the Sn isotopes. Data from the latter experiment are available in an energy range 6 – 20 MeV, covering the major part of the IVGDR and providing sufficient overlap with the Oslo method results. It should be noted that previous photoabsorption experiments using the ( $\gamma, xn$ ) reaction show considerable scatter in the systematics of IVGDR parameters. In contrast, the results of Ref. [25] provide centroid energies in line with empirical systematics and an almost constant width, as expected from the similar g.s. structure. In the energy region close to  $S_n$ , where discrepancies with older data are particularly pronounced, they are also in good agreement with new ( $\gamma, n$ ) experiments [47, 48] using monoenergetic photon beams from laser Compton back-scattering.

## 3. Decomposition of the low-energy electric dipole strength

A decomposition of the LEDS is performed for the example of  $^{124}\text{Sn}$  illustrated in Fig. 1. The following contributions to the total GSF are considered: a low-energy tail of the IVGDR, a spin-flip  $M1$  resonance, an upbend at very low energies and one or two (when demanded by the data)  $E1$  resonances. The generalized Lorentzian model (solid blue line in Fig. 1) is chosen

to describe the IVGDR part [49]

$$f_{\text{IVGDR}}(E_\gamma) = \frac{1}{3\pi^2 \hbar^2 c^2} \sigma_{\text{IVGDR}} \Gamma_{\text{IVGDR}} \times \left[ E_\gamma \frac{\Gamma_{\text{KMF}}(E_\gamma, T_f)}{(E_\gamma^2 - E_{\text{IVGDR}}^2)^2 + E_\gamma^2 \Gamma_{\text{KMF}}^2(E_\gamma, T_f)} + 0.7 \frac{\Gamma_{\text{KMF}}(E_\gamma = 0, T_f)}{E_{\text{IVGDR}}^3} \right] \quad (1)$$

with  $E_{\text{IVGDR}}$ ,  $\Gamma_{\text{IVGDR}}$ ,  $\sigma_{\text{IVGDR}}$  being the IVGDR centroid energy, width, and maximum cross section, respectively.  $\Gamma_{\text{KMF}}$  corresponds to a temperature-dependent width in the Kadenskii-Markushev-Furman model [50], where  $T_f$  refers to final states. It is the only empirical or microscopic model capable of accounting simultaneously for the low-energy flank of the IVGDR and a relatively flat strength distribution at very low energies (2 – 4 MeV).

Data on the M1 spin-flip resonance are available (green points) in the energy region from 6 to about 12 MeV from Ref. [25] and show broad distributions. They are parameterized by a single Lorentzian (dashed green line). The upbend at very low energies is described by exponential functions (dashed gray line). The determination of parameters is described in Ref. [38], but its details have no influence on the present results. Finally, additional resonances on top of the tail of the IVGDR are assumed to be Gaussian (shaded red and violet areas). All parameters are determined by a simultaneous fit (dark red line) to the combined Oslo (blue points and error band) and  $(p, p')$  (orange points and error band) data described above. An in-depth discussion of the decomposition is provided in Ref. [38].

Figure 2 presents the evolution of the LEDS and its various components with mass number when integrating within the 4 – 10 MeV energy region. The total LEDS is roughly constant (with slight indications of a local maximum at  $^{120}\text{Sn}$ ) with values ranging from 3.5% to 4% of the classical Thomas-Reiche-Kuhn (TRK) sum rule. The contribution of the low-energy tail of the IVGDR is found to be approximately constant as well as exhausting a TRK value of about 1.5%. The strength on top of the tail of the IVGDR in the isotopes with  $A \leq 118$  is well parameterized by a single Gaussian function. For  $A \geq 118$  the  $(p, p')$  data demand the inclusion of a second peak at lower energies, which is particularly pronounced in  $^{124}\text{Sn}$  (cf. Fig. 1). The dominant peak is centered at about 8.3 MeV and its average strength is 2% of the TRK value. Small variations are visible as a function of mass number with a possible strength maximum at  $^{120}\text{Sn}$ . A similar local maximum of the LEDS at  $^{120}\text{Sn}$  has been discussed e.g. in Refs. [1, 6, 51].

The centroid of the lower-energy peak lies at about 6.5 MeV with no energy dependence within uncertainties. Its strength is small, ranging from 0.1% for  $^{118}\text{Sn}$  to a maximum of 0.5% of the TRK sum rule in  $^{124}\text{Sn}$ . Interestingly, this contribution shows an approximately linear dependence on mass number (or neutron excess). When extrapolated to lower masses, its predicted strength is too small to be distinguished from the broad peak at higher energies. Studies of the isoscalar E1 strength in  $^{124}\text{Sn}$  with the  $(\alpha, \alpha'\gamma)$  [19, 24] and  $(^{17}\text{O}, ^{17}\text{O}'\gamma)$  [21] reactions show a concentration between 5.5 and 7 MeV, consistent with

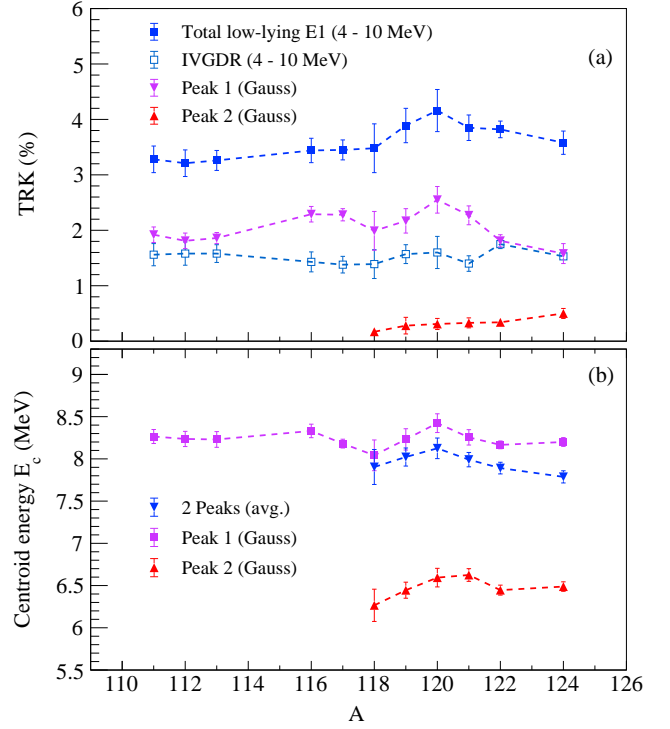


Figure 2: Systematics of the total LEDS integrated over the energy region 4 – 10 MeV and its decomposition into the contributions from the tail of the IVGDR and one or two (for masses  $\geq 118$ ) resonances on top. (a) Strengths in % of the TRK sum rule. (b) centroid energies.

the properties of the lower-energy peak. Furthermore, studies of the  $^{112,116,120,124}\text{Sn}(\gamma, \gamma')$  reaction [28, 29] typically find the strongest transitions between 6 and 7 MeV, indicating large g.s. branching ratios. These experimental signatures point towards an interpretation of the lower-energy peak as the IV response of the PDR.

These numbers are significantly smaller than quoted in most theoretical studies of the dependence of the PDR strength on neutron excess in the Sn isotope chain (for a notable exception see Ref. [8]). They challenge an interpretation of the PDR as neutron skin oscillation, which implies some degree of collectivity. Of course, the distinction of strength belonging either to the PDR or to the tail of the IVGDR is schematic. In reality, there is some degree of mixing between transitions of different types. All QRPA calculations agree on a gradual change of the radial transition densities from an approximate IS behavior in the interior of the nucleus and a pronounced peak of the neutron density at the surface (a signature of the PDR) to more IV-type transitions at higher energies. However, for the confined energy region where the PDR strength is located, effects on the IV response due to variations of the transition densities are expected to be small.

The discrepancy probably arises in many cases from the fact that QRPA results typically produce a single low-energy peak and its strength is assumed to represent the PDR strength. The present work and experiments comparing the IS and IV response on the same nucleus demonstrate that this is *not* correct.

The PDR strength exhausts a rather small fraction of the LEDS only (at most about 15% for the Sn isotopes studied here). Thus, quantitative predictions based on QRPA have to be taken with some care, and one might have to go beyond it by including complex configurations to achieve realistic low-energy strength distributions. This is discussed in the next section.

#### 4. Comparison with *ab initio*-based microscopic calculations

In the following we compare the experimental GSFs with *ab initio*-based microscopic calculations using  $^{120}\text{Sn}$  as a representative example. An extensive discussion of the models and a comparison with all experimental results can be found in Ref. [38]. Nuclear response theory can be consistently derived in the model-independent *ab initio* equation of motion (EOM) framework [52, 53, 54] for the in-medium two-time two-fermion propagators. In superfluid media, particle-hole (*ph*), particle-particle (*pp*), and hole-hole (*hh*) propagators can be conveniently unified in one two-quasiparticle (*2q*) propagator without loss of generality [55].

While the generic EOM for the correlated (four-time) two-fermion propagator is the Bethe-Salpeter equation, the two-time character of the response leads to the EOM of a Dyson form, which depends on a single time difference. The interaction kernel of the Bethe-Salpeter-Dyson equation, before taking any approximation, decomposes into the static and dynamical (time-dependent) components. In the energy domain, they are represented by the energy-independent and energy-dependent terms, respectively. The energy-dependent contribution generates long-range correlations while making an impact on their short-range static counterpart. Since the *2q* EOM couples to a growing hierarchy of higher-rank EOMs via the dynamical kernel, in practical applications it is decoupled by making approximations with varying correlation content.

The simplest decoupling scheme retains only the static kernel and is known as the quasiparticle random phase approximation (QRPA). The heart of the dynamical kernel is the four-fermion *4q* fully correlated propagator contracted with two interaction matrix elements. The approximation keeping the leading effects of emergent collectivity in the *4q* propagator reduces it to *2q*  $\otimes$  *phonon* configurations, where the *phonon* represents correlated *2q* pairs (vibrations). This approach reproduces the phenomenological (relativistic) quasiparticle time-blocking approximation ((R)QTBA) [56, 57] if the bare interaction between nucleons is replaced by their effective interaction. However, in the *ab initio* EOM method, the quasiparticle-vibration coupling (qPVC) amplitudes are derived consistently from the underlying interaction, while in (R)QTBA the qPVC self-energy is used as an input. The EOM works with the two-time propagators from the beginning and hence does not employ time blocking. Furthermore, the *ab initio* relativistic EOM (REOM) framework links the nuclear response theory to the underlying scale of particle physics and fundamental interactions, in the present case, to the meson-exchange interaction and, more importantly, enables extensions of the *4q* dynamical kernel to more complex configurations [55].

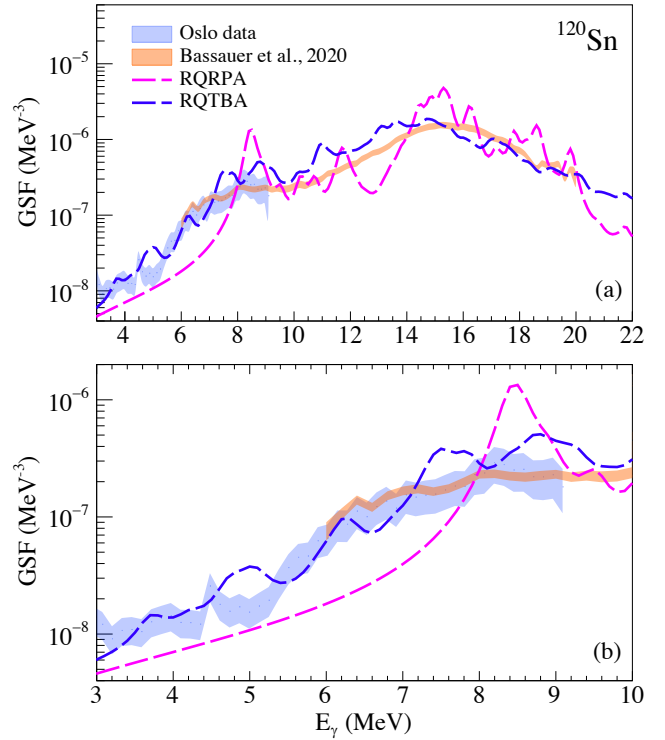


Figure 3: Comparison of experimental and calculated GSFs computed with an artificial width of 200 keV for  $^{120}\text{Sn}$  in the energy regions (a) 4 – 22 MeV and (b) 3 – 10 MeV. The blue and orange bands indicate the Oslo-method and (*p*, *p'*) data. The RQRPA and RQTBA calculations described in the text are shown as magenta and violet lines, respectively.

The cluster decomposition of this kernel identifies the next-level complexity non-perturbative approximation as the *2q*  $\otimes$  *2phonon*. The implementation of such configurations is becoming gradually possible with the increasing computational capabilities [54, 58] and will be applied for systematic calculations in the near future. While implementations with bare interactions are not yet available, (R)EOM admits realistic implementations that employ effective interactions adjusted in the framework of the density functional theory. For such interactions, the qPVC in the dynamical kernel can be combined with subtraction, restoring the self-consistency of the *ab initio* framework [59], while reasonable phonons can be obtained already on the QRPA level.

In this work, the effective meson-exchange interaction NL3\* [60] was employed. This interaction has a transparent link to particle physics, while the meson masses and coupling constants are only slightly different from their vacuum values (cf., for instance, Ref. [61]). The NL3\* is an upgraded version of the previously developed NL3 parametrization [62], which includes self-interactions in the scalar  $\sigma$  meson sector [63]. The self-interactions represent three and four  $\sigma$  meson vertices, i.e., concrete physical processes that occur in correlated media. The NL3 and NL3\* ansätze are separable in the momentum representation, which speeds up the computation considerably. With these interactions, the realization of the REOM approach on the

$2q \otimes \text{phonon}$  level technically corresponds to RQTBA, so this name is retained in the present work.

Results of the RQRPA and RQTBA calculations for the electric dipole strength in  $^{120}\text{Sn}$  are displayed in Fig. 3 together with the data. The  $(p, p')$  results in the energy region of the IVGDR (orange band in Fig. 3(a)), are reasonably well described by both approaches. The successful reproduction of the gross features by the RQRPA calculations highlights the importance of Landau damping for an understanding of IVGDR widths in heavy nuclei [64]. An expanded view of the low-energy region is given in Fig. 3(b), where significant differences between the RQRPA and RQTBA results are apparent. With RQRPA, the LEDS is concentrated in a single transition at 8.6 MeV. The strength at lower energies is an artefact of the 200 keV width in the calculations only. Inclusion of qPVC provides a satisfactory description of the energy dependence of the LEDS on a quantitative level down to energies of about 3 MeV. The experimental structure centered at 8.5 MeV in  $^{120}\text{Sn}$ , cf. Fig. 2(b), is split in the RQTBA results into two major contributions at 7.8 and 8.8 MeV. A structure corresponding to the lower-energy peak at 6.5 MeV is also visible. Some local deviation is seen around 5 MeV. However, as discussed above, including  $2q \otimes 2\text{phonon}$  configurations as the next level of complexity promises to bring the theoretical results in even better agreement with the data, in particular at lower energies.

The differences in the description of the LEDS underline the problems of an interpretation of the PDR based on calculations on the QRPA level. The predicted strengths correspond to the total LEDS rather than the PDR, and the latter carries a small fraction only. Thus, an analysis of the structures underlying the PDR and the dominant IV resonance at higher energies based on mean-field models should include qPVC, at least in the leading approximation.

The agreement of RQTBA to the experimental LEDS data, although significantly improved compared to RQRPA, is still imperfect. This is illustrated in Fig. 4, where the experimental and theoretical strengths integrated between 4 and 10 MeV are compared as functions of mass number. Both model results show a monotonous increase between mass numbers 112 and 124 from about 1.5% to 7.5% of the TRK sum rule for RQRPA and 2.5% to 6.5% for RQTBA, respectively. In contrast, the experimental strengths are approximately constant with values 3.5–4%. For the case of  $^{120}\text{Sn}$ , the models predict extra strength compared to the data in the energy region 7 – 10 MeV, leading to a total value of 6%. This indicates that some mechanisms of the strength formation are still missing to achieve spectroscopic accuracy. A complete response theory should take into account the continuum, including the multiparticle escape, a more complete set of phonons (in particular, those of unnatural parity and isospin-flip), complex ground-state correlations, and higher-complexity configurations.

## 5. Summary and conclusions

We present a systematic study of the low-energy electric dipole strength in Sn isotopes ranging from  $A = 111$  to 124 based on the data for  $^{111-113,116,118-122,124}\text{Sn}$  obtained with the

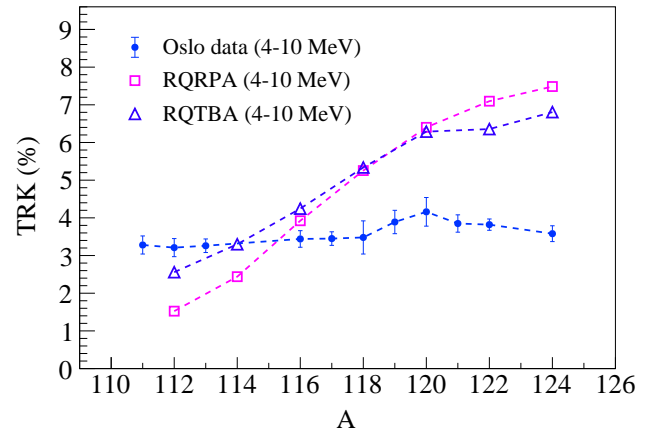


Figure 4: Evolution of the experimental LEDS in the energy range 4–10 MeV for Sn isotopes with mass numbers  $A = 111$ –124 compared with predictions of the RQRPA (open squares) and RQTBA (open triangles) calculations described in the text. The dashed lines are to guide the eye.

Oslo method and the study of  $^{112,114,116,118,120,124}\text{Sn}$  with relativistic Coulomb excitation in forward angle  $(p, p')$  scattering. The tin chain is of particular interest since the similarity of low-energy structure in the neighboring isotopes allows to single out the impact of neutron excess on the evolution of the LEDS. The combined data cover an energy range of 2 – 20 MeV which permits a decomposition into the contribution from the low-energy tail of the IVGDR and possible resonance-like structures with minimal assumptions. One finds in all cases a resonance at about 8.3 MeV, exhausting an approximately constant fraction of the TRK sum rule with a local maximum at  $^{120}\text{Sn}$  which might be attributed to shell structure effects.

For the isotopes with  $A \geq 118$ , a consistent description of the data suggests introducing a second resonance centered at about 6.5 MeV. The comparison with the results from the isoscalar probes and the  $(\gamma, \gamma')$  reaction indicates that it might represent the IV response of the PDR. Its strength corresponds to a relatively small fraction of the total LEDS and demonstrates an approximately linear dependence on mass number. Because of the schematic decomposition into contributions from the IVGDR and resonances, the absolute values might have some model dependence. Nevertheless, these results demonstrate that taking the full LEDS as representative for the PDR strength (as done in many discussions of a possible relation to the neutron skin thickness) is clearly unfounded. The small PDR strength also challenges its interpretation of being due to neutron skin oscillations, which requires some degree of collectivity. However, this question cannot be settled based on the IV response alone.

Microscopic calculations rooted in ab initio EOM theory can reproduce the experimental features in  $^{120}\text{Sn}$  remarkably well, provided qPVC is included. Consideration of qPVC generally improves the description of the LEDS (cf. Ref. [38]). However, even in the latter case, calculations are still failing to reproduce the experimental mass dependence of the LEDS. While the experimental strengths are roughly constant, the theoretical results

predict a monotonous increase with mass number.

Further work is required to elucidate the true nature of the PDR. One way are systematic studies of the IV and IS response along isotopic or isotonic chains, similar to the one presented here. For the Sn case, experiments at RIB facilities in inverse kinematics, analogous to the pioneering study of E1 strength in  $^{130,132}\text{Sn}$  [65], but including the information on  $\gamma$  decay [66, 67] to extract the GSF below neutron thresholds, would be of particular interest. New experimental observables like the particle-hole structure investigated in transfer reactions [68, 69] or transition current densities from transverse electron scattering [23] may help to clarify the underlying structure. Theoretically, the role of the continuum, inclusion of more complete sets of phonons, and in particular the impact of 6-quasiparticle configurations need to be investigated.

## Acknowledgements

This work was supported in part by the National Science Foundation under Grant No. OISE-1927130 (IRENA) and by the Norwegian Research Council Grants 325714 and 263030. P.v.N.-C. acknowledges support by the Deutsche Forschungsgemeinschaft (DFG, German Research Foundation) under Grant No. SFB 1245 (Project ID 279384907). The work of E.L. was supported by the GANIL Visitor Program, US-NSF Grant PHY-2209376, and US-NSF Career Grant PHY-1654379.

## References

- [1] N. Paar, et al., Rep. Prog. Phys. 70 (2007) 671, <http://dx.doi.org/10.1088/0034-4885/70/5/R02>.
- [2] D. Savran, et al., Prog. Part. Nucl. Phys. 70 (2013) 210, <http://dx.doi.org/10.1016/j.pnpnp.2013.02.003>.
- [3] A. Bracco, et al., Prog. Part. Nucl. Phys. 106 (2019) 360, <http://dx.doi.org/10.1016/j.pnpnp.2019.02.001>.
- [4] E. Lanza, et al., Prog. Part. Nucl. Phys. 129 (2023) 104006, <http://dx.doi.org/10.1016/j.pnpnp.2022.104006>.
- [5] S. Goriely, Eur. Phys. J. A 59 (2023) 16, <http://dx.doi.org/10.1140/epja/s10050-023-00931-x>.
- [6] J. Piekarewicz, Phys. Rev. C 73 (2006) 044325, <http://dx.doi.org/10.1103/PhysRevC.73.044325>.
- [7] A. Klimkiewicz, et al., Phys. Rev. C 76 (2007) 051603, <http://dx.doi.org/10.1103/PhysRevC.76.051603>.
- [8] N. Tsoneva, H. Lenske, Phys. Rev. C 77 (2008) 024321, <http://dx.doi.org/10.1103/PhysRevC.77.024321>.
- [9] A. Carbone, et al., Phys. Rev. C 81 (2010) 041301, <http://dx.doi.org/10.1103/PhysRevC.81.041301>.
- [10] J. Piekarewicz, Phys. Rev. C 83 (2011) 034319, <http://dx.doi.org/10.1103/PhysRevC.83.034319>.
- [11] S. Ebata, et al., Phys. Rev. C 90 (2014) 024303, <http://dx.doi.org/10.1103/PhysRevC.90.024303>.
- [12] V. Baran, et al., Eur. Phys. J. D 68 (2014) 356, <http://dx.doi.org/10.1140/epjd/e2014-50171-x>.
- [13] E. Litvinova, et al., Phys. Rev. C 79 (2009) 054312, <http://dx.doi.org/10.1103/PhysRevC.79.054312>.
- [14] P.-G. Reinhard, W. Nazarewicz, Phys. Rev. C 81 (2010) 051303, <http://dx.doi.org/10.1103/PhysRevC.81.051303>.
- [15] M. Urban, Phys. Rev. C 85 (2012) 034322, <http://dx.doi.org/10.1103/PhysRevC.85.034322>.
- [16] P.-G. Reinhard, W. Nazarewicz, Phys. Rev. C 87 (2013) 014324, <http://dx.doi.org/10.1103/PhysRevC.87.014324>.
- [17] P. Papakonstantinou, et al., Phys. Rev. C 89 (2014) 034306, <http://dx.doi.org/10.1103/PhysRevC.89.034306>.
- [18] D. Savran, et al., Phys. Rev. Lett. 97 (2006) 172502, <http://dx.doi.org/10.1103/PhysRevLett.97.172502>.
- [19] J. Endres, et al., Phys. Rev. Lett. 105 (2010) 212503, <http://dx.doi.org/10.1103/PhysRevLett.105.212503>.
- [20] F. C. L. Crespi, et al., Phys. Rev. Lett. 113 (2014) 012501, <http://dx.doi.org/10.1103/PhysRevLett.113.012501>.
- [21] L. Pellegri, et al., Phys. Lett. B 738 (2014) 519, <http://dx.doi.org/10.1016/j.physletb.2014.08.029>.
- [22] A. Repko, et al., Eur. Phys. J. A 55 (2019) 242, <http://dx.doi.org/10.1140/epja/i2019-12770-x>.
- [23] P. von Neumann-Cosel, et al., <http://dx.doi.org/10.48550/arXiv.2310.04736> (2023).
- [24] J. Endres, et al., Phys. Rev. C 85 (2012) 064331, <http://dx.doi.org/10.1140/10.1103/PhysRevC.85.064331>.
- [25] S. Bassauer, et al., Phys. Rev. C 102 (2020) 034327, <http://dx.doi.org/10.1103/PhysRevC.102.034327>.
- [26] A. Krumbholz, et al., Phys. Lett. B 744 (2015) 7, <http://dx.doi.org/10.1016/j.physletb.2015.03.023>.
- [27] P. von Neumann-Cosel, A. Tamii, Eur. Phys. J. A 55 (2019) 110, <http://dx.doi.org/10.1140/epja/i2019-12781-7>.
- [28] B. Özel-Tashenov, et al., Phys. Rev. C 90 (2014) 024304, <http://dx.doi.org/10.1103/PhysRevC.90.024304>.
- [29] K. Govaert, et al., Phys. Rev. C 57 (1998) 2229, <http://dx.doi.org/10.1103/PhysRevC.57.2229>.
- [30] A. Zilges, other, Prog. Part. Nucl. Phys. 122 (2022) 103903, <http://dx.doi.org/10.1016/j.pnpnp.2021.103903>.
- [31] M. Müscher, et al., Phys. Rev. C 102 (2020) 014317, <http://dx.doi.org/10.1103/PhysRevC.102.014317>.
- [32] M. Markova, et al., Phys. Rev. Lett. 127 (2021) 182501, <http://dx.doi.org/10.1103/PhysRevLett.127.182501>.
- [33] M. Markova, et al., Phys. Rev. C 106 (2022) 034322, <http://dx.doi.org/10.1103/PhysRevC.106.034322>.
- [34] M. Markova, et al., Phys. Rev. C 108 (2023) 014315, <http://dx.doi.org/10.1103/PhysRevC.108.014315>.
- [35] S. Bassauer, et al., Phys. Lett. B 810 (2020) 135804, <http://dx.doi.org/10.1016/j.physletb.2020.135804>.
- [36] D. M. Brink, doctoral thesis, Oxford University (1955).
- [37] P. Axel, Phys. Rev. 126 (1962) 671, <http://dx.doi.org/10.1103/physrev.126.671>.
- [38] M. Markova, et al., <http://dx.doi.org/10.48550/arXiv.2311.08864> (2023).
- [39] M. Guttormsen, et al., Nucl. Instrum. Methods Phys. Res. A 648 (2011) 168, <http://dx.doi.org/10.1016/j.nima.2011.05.055>.
- [40] M. Guttormsen, et al., Phys. Scr. T32 (1990) 54, <http://dx.doi.org/10.1088/0031-8949/1990/T32/010>.
- [41] V. W. Ingeberg, et al., Eur. Phys. J. A 56 (2020) 68, <http://dx.doi.org/10.1140/epja/s10050-020-00070-7>.
- [42] F. Zeiser, et al., Nucl. Instrum. Methods Phys. Res. A 985 (2021) 164678, <http://dx.doi.org/10.1016/j.nima.2020.164678>.
- [43] L. Netterdon, et al., Phys. Lett. B 744 (2015) 358, <http://dx.doi.org/10.1016/j.physletb.2015.04.018>.
- [44] M. Guttormsen, et al., Phys. Rev. Lett. 116 (2016) 012502, <http://dx.doi.org/10.1103/PhysRevLett.116.012502>.
- [45] D. Martin, et al., Phys. Rev. Lett. 119 (2017) 182503, <http://dx.doi.org/10.1103/PhysRevLett.119.182503>.
- [46] J. Isaak, et al., Phys. Lett. B 788 (2019) 225, <http://dx.doi.org/10.1016/j.physletb.2018.11.038>.
- [47] H. Utsunomiya, et al., Phys. Rev. C 80 (2009) 055806, <http://dx.doi.org/10.1103/PhysRevC.80.055806>.
- [48] H. Utsunomiya, et al., Phys. Rev. C 84 (2011) 055805, <http://dx.doi.org/10.1103/PhysRevC.84.055805>.
- [49] R. Capote, et al., Nucl. Data Sheets 110 (2009) 3107, <http://dx.doi.org/10.1016/j.nds.2009.10.004>.
- [50] S. Kadmenskii, et al., Sov. J. Nucl. Phys. 37 (1983) 345, [http://inis.iaea.org/search/search.aspx?orig\\_q=RN:15008335](http://inis.iaea.org/search/search.aspx?orig_q=RN:15008335).
- [51] S. Burrello, et al., Phys. Rev. C 99 (2019) 054314, <http://dx.doi.org/10.1103/PhysRevC.99.054314>.
- [52] S. Adachi, P. Schuck, Nucl. Phys. A496 (1989) 485, [http://dx.doi.org/10.1016/0375-9474\(89\)90073-0](http://dx.doi.org/10.1016/0375-9474(89)90073-0).
- [53] J. Dukelsky, et al., Nucl. Phys. A628 (1998) 17, [http://dx.doi.org/10.1016/S0375-9474\(97\)00606-4](http://dx.doi.org/10.1016/S0375-9474(97)00606-4).

- [54] E. Litvinova, P. Schuck, Phys. Rev. C 100 (2019) 064320, <http://dx.doi.org/10.1103/PhysRevC.100.064320>.
- [55] E. Litvinova, Y. Zhang, Phys. Rev. C 106 (2022) 064316, <http://dx.doi.org/10.1103/PhysRevC.106.064316>.
- [56] V. I. Tselyaev, Phys. Rev. C 75 (2007) 024306, <http://dx.doi.org/10.1103/PhysRevC.75.024306>.
- [57] E. Litvinova, et al., Phys. Rev. C 78 (2008) 014312, <http://dx.doi.org/10.1103/PhysRevC.78.014312>.
- [58] E. Litvinova, <http://dx.doi.org/10.48550/arXiv.2308.07574> (2023).
- [59] V. I. Tselyaev, Phys. Rev. C 88 (2013) 054301, <http://dx.doi.org/10.1103/PhysRevC.88.054301>.
- [60] G. A. Lalazissis, et al., Phys. Lett. B 671 (2009) 36, <http://dx.doi.org/10.1016/j.physletb.2008.11.070>.
- [61] R. Machleidt, Adv. Nucl. Phys. 19 (1989) 189, [http://dx.doi.org/10.1007/978-1-4613-9907-0\\_2](http://dx.doi.org/10.1007/978-1-4613-9907-0_2).
- [62] G. Lalazissis, J. König, P. Ring, Phys. Rev. C 55 (1997) 540–543, <http://dx.doi.org/10.1103/PhysRevC.55.540>.
- [63] J. Boguta, A. Bodmer, Nucl. Phys. A 292 (1977) 413, [http://dx.doi.org/10.1016/0375-9474\(77\)90626-1](http://dx.doi.org/10.1016/0375-9474(77)90626-1).
- [64] P. von Neumann-Cosel, V. Ponomarev, A. Richter, J. Wambach, Eur. Phys. J. A 55 (2019) 224, <http://dx.doi.org/10.1140/epja/i2019-12795-1>.
- [65] P. Adrich, et al., Phys. Rev. Lett. 95 (2005) 132501, <http://dx.doi.org/10.1103/PhysRevLett.95.132501>.
- [66] O. Wieland, et al., Phys. Rev. Lett. 102 (2009) 092502, <http://dx.doi.org/10.1103/PhysRevLett.102.092502>.
- [67] D. M. Rossi, et al., Phys. Rev. Lett. 111 (2013) 242503, <http://dx.doi.org/10.1103/PhysRevLett.111.242503>.
- [68] M. Spieker, et al., Phys. Rev. Lett. 125 (2020) 102503, <http://dx.doi.org/10.1103/PhysRevLett.125.102503>.
- [69] M. Weinert, et al., Phys. Rev. Lett. 127 (2021) 242501, <http://dx.doi.org/10.1103/PhysRevLett.127.242501>.